ACS APPLIED MATERIALS & INTERFACES

Letter

www.acsami.org

Cell Membrane Tracker Based on Restriction of Intramolecular Rotation

Chunqiu Zhang,[†,‡] Shubin Jin,[†,‡] Keni Yang,[†] Xiangdong Xue,[†] Zhipeng Li,[†] Yonggang Jiang,[†] Wei-Qiang Chen,[‡] Luru Dai,[†] Guozhang Zou,*[,†] and Xing-Jie Liang*[,†]

[†]CAS Key Laboratory for Biological Effects of Nanomaterials & Nanosafety, National Center for Nanoscience and Technology, No. 11 Beiyitiao, Zhongguancun, Beijing 100190, China

[‡]Institute of Modern Physics, Chinese Academy of Sciences, Lanzhou 730000, China

Supporting Information

ABSTRACT: The fluorescence of tetraphenylethylene (TPE), an archetypal luminogen, is induced by restriction of intramolecular rotation (RIR). TPE was grafted with palmitic acid (PA) onto a hydrophilic peptide to yield a cell membrane tracker named TR4. TR4 was incorporated into liposomes, where it showed significant RIR characteristics. When cells were incubated with TR4, cytoplasmic membranes were specifically labeled. TR4 shows excellent photostability and low cytotoxicity.

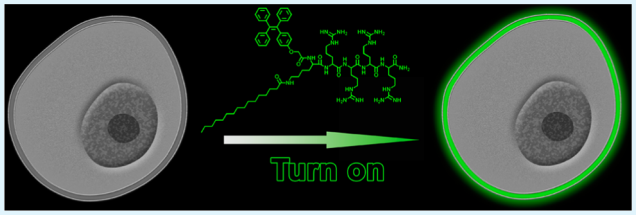

KEYWORDS: *cell membrane, tracker, tetraphenylethylene (TPE), restriction of intramolecular rotation (RIR)*

The cytoplasmic membrane is the two-dimensional boundary between a living cell and its environment. Cytoplasmic membrane-related events, including dynamic membrane remodeling, signal transduction, and nutrient transport, are of great interest to cell biologists. To study these events, it is very important to develop probes for subcellular fluorescence imaging that can identify the cytoplasmic membrane and record the dynamic changes.[1,2] Until now, there have bene only a few commercial fluorescent dyes available for tracking cell membranes, such as DiO[3] and DiI.[4] Typically, these probes have a lipophilic structure that allows them to become embedded into cell membranes; however, they generate background fluorescence even when they do not bind to cell membranes, resulting in a low signal-to-noise (S/N) ratio. In addition, they are susceptible to photobleaching under laser exposure, which means they are not suitable for long-term observation or real-time tracking. Fluorescently labeled proteins, such as labeled lectins that bind to cell surface sugars, are an alternative type of membrane probe. However, these probes result in inconsistent staining with variation across cell types. Therefore, it is desirable to develop new photostable fluorescent probes that specifically and consistently stain the cell membrane with low background.

Recently, the unique phenomenon of aggregation-induced emission (AIE) has attracted more and more attention for the design of novel fluorescent probes.[5−7] TPE, an archetypal AIE luminogen, has been widely used to develop "turn on" fluoresecent chemosensors,[8] bioprobes,[9−13] and optoelectronic materials.[14−18] The AIE mechanism is due to the restriction of intermolecular rotation (RIR),[19,20] which prohibits energy dissipation and leads to high quantum yield. In contrast to conventional fluorescent dyes, AIE luminogens exhibit bright emission in the aggregated state, when intramolecular motion is hindered, but no or very weak emission in the monodisperse state, when intramolecular motion is unrestricted.[21,22] Alternatively, because of the RIR effect, AIE luminogens can become highly fluorescent when individually dispersed molecules are entrapped in a tight space, even though no aggregation happens.[23] To date, a number of bioprobes have been developed on the basis of this AIE mechanism, but only four AIE dyes have been developed to track specific organelles in the cell.[24−27] Thus, we set out to design a novel cell membrane tracker based on an AIE luminogen that displays the RIR effect.

In the search for an alternative cell membrane tracker, we designed and constructed an amphipathic molecule, TR4, as shown in Figure 1. First, the molecule has a short tetra-peptide sequence consisting of four arginine residues as the positively charged hydrophilic moiety to target membranes. Second, inspired by the structure of DiI, as shown in Figure 1A, palmitic acid (PA) and tetraphenylethylene (TPE) were conjugated to the peptide to provide a lipophilic moiety for membrane insertion. Third, the TPE was employed to "turn on" luminescence upon being embedded in the membrane. The probe, as designed, can bind to the lipid bilayers of liposomes, where it displays bright fluorescence. When applied to actual living cells, TR4 exhibited low toxicity and specifically labeled the cytoplasmic membrane (Figure 1B). Compared to the commercial dye DiI, our probe showed remarkable photostability, and can be used for long-term real-time tracking. In

Received: April 28, 2014
Accepted: May 30, 2014
Published: May 30, 2014

   dx.doi.org/10.1021/am5025897 | ACS Appl. Mater. Interfaces 2014, 6, 8971−8975

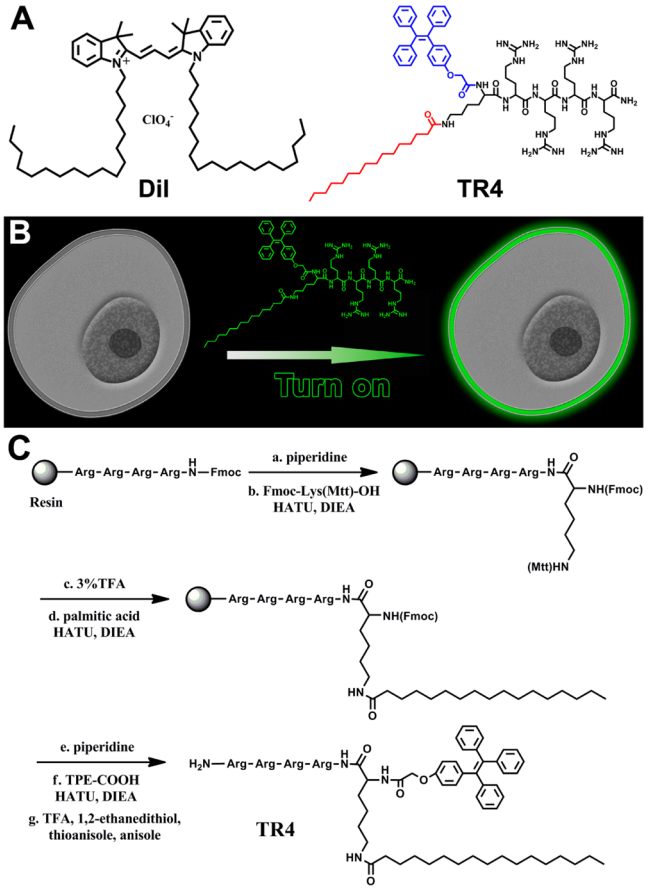

Figure 1. (A) Molecular structures of DiI and TR4; (B) schematic illustration of the targeted labeling of the cell membrane by TR4; (C) synthetic scheme of amphiphilic TR4.

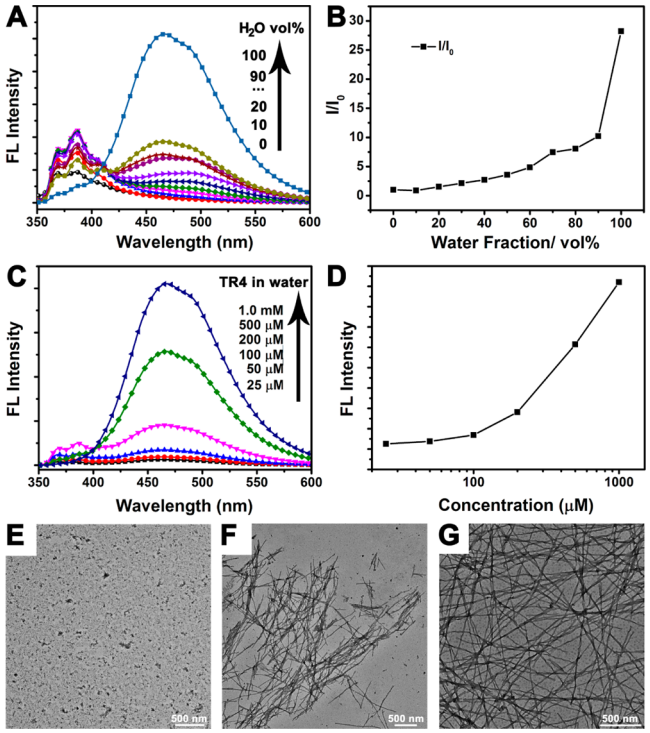

Figure 2. (A) Fluorescence spectra of TR4 (500 μM) in DMF/water mixtures with different water fractions (vol %). (B) plot of fluorescence intensity (I) of TR4 (500 μM) at 466 nm versus the water fraction of the DMF/water mixture. I_0 = fluorescence intensity of TR4 in pure DMF solution (λ_{ex} = 330 nm). (C) Fluorescence spectra of TR4 at different concentrations (25 μM to 1.0 mM) in water. (D)Plot of peak fluorescence intensity (466 nm) of TR4 in water versus concentration (λ_{ex} = 330 nm); TEM images of nanostructures of (E) TR4 (100 μM), (F) TR4 (200 μM), and (G) TR4 (500 μM) in water.

addition, our probe can be excited by two photons of infrared light, which is very attractive for two-photon microscopy.

To synthesize this bioprobe, carboxylated tetraphenylethylene (TPE-COOH) was synthesized as a building block.[14] The designed probe could then be easily obtained by solid-phase peptide synthesis (SPPS) (Figure 1C). The molecular weight of TR4 was determined by MALDI-TOF-MS (see the Supporting Information, Figure S1) and the purity was verified by reverse-phase HPLC (see the Supporting Information, Figure S2). In the benign solvent (DMF), TR4 (500 μM) showed no fluorescence. However, when H_2O was added into the DMF solution so that the fraction was above 90% (volume%), the fluorescence intensity of TR4 (500 μM) increased dramatically (Figure 2A, B). As expected, the fluorescence was turned on by AIE. When TR4 was added to water at low concentrations (<200 μM), it dissolved completely and existed as monodispersed molecules because of the presence of the hydrophilic moiety formed by the four arginine residues. At concentrations of 200 μM and above, the TR4 solution turned fluorescent, as shown in Figure 2C and D, indicative of aggregate formation. To confirm this mechanism, we investigated the morphology of TR4 at different concentrations by transmission electron microscopy (TEM). As shown in Figure 2E, no typical nanostructures were observed when the concentration of TR4 was 100 μM. Consistent with the fluorescence measurements, TR4 self-assembled to form some short nanofibers when the concentration was raised to 200 μM (Figure 2F). At 500 μM, TR4 formed a greater number of longer nanofibers (Figure 2G). These results were consistent with the observed AIE fluorescence of TR4 in aqueous solution, i.e. the bright fluorescence was induced by the self-assembly of TR4. The results also prompted us to use TR4 at a working concentration below 100 μM for our next experiment, in order to keep the probe in its monodisperse state and to eliminate background fluorescence.

To test whether the probe can bind to lipid membranes, we prepared liposomes and investigated whether TR4 could insert into the amphiphilic lipid bilayer. TR4-free liposomes with a diameter of about 100 nm were prepared by mixing hydrogenated phosphatidylcholine (hsPC) and cholesterol (see the Supporting Information, Figure S3). The cholesterol was used to stabilize the liposomes. TR4-loaded liposomes (TR4@liposomes) were then fabricated by incubating TR4 (10−100 μM) with the liposomes for 30 min. As shown in Figure 3A and B, the emission from the TR4@liposomes was enhanced as the concentration of TR4 increased. Typically, the emission of TR4 (50 μM) in water remained rather weak; however, the turned-on fluorescence of TR4@liposomes (50 μM) was observed under a 365 nm lamp and verified by fluorescence spectroscopy (Figure 3C). Next, the integrity of TR4@liposomes was investigated by TEM. As shown in Figure 3D, the morphology of TR4@liposomes was not changed, indicating that the insertion of TR4 did not disturb the structure of the liposomes, even though the FL intensity of TR4

dx.doi.org/10.1021/am5025897 | ACS Appl. Mater. Interfaces 2014, 6, 8971−8975

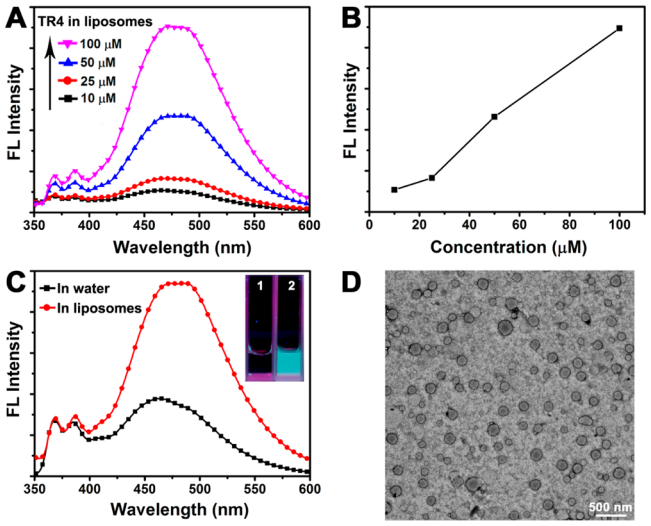

Figure 3. (A) Fluorescence spectra of TR4 embedding into liposomes, where the concentration of TR4 ranged from 10 μM to 100 μM. (B) Plot of fluorescence intensity of liposomes in the presence of TR4 at 466 nm versus concentration (λ_{ex} = 330 nm). (C) Fluorescence spectra of TR4 (50 μM) in water or in liposomes. Inset: photograph showing fluorescence of TR4 in water (1), and TR4 in liposomes (2) under UV light (365 nm). (D) TEM image of liposomes in the presence of TR4 (50 μM).

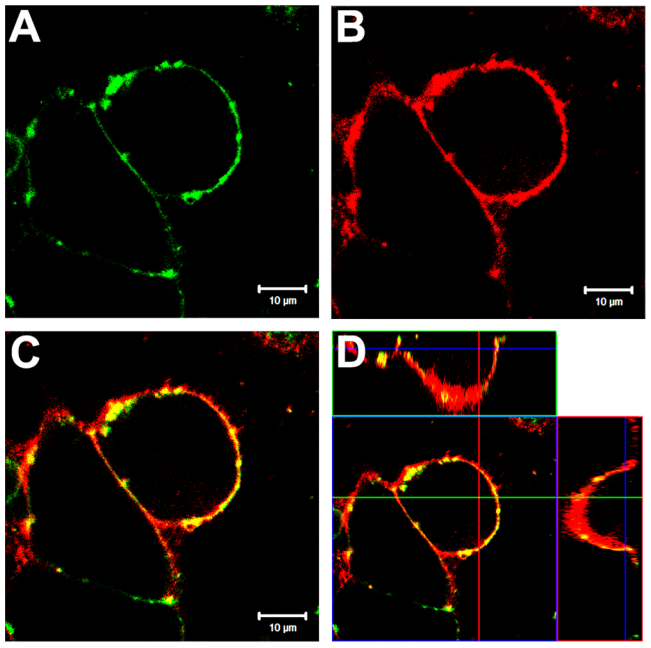

Figure 4. Living MCF-7 cells were incubated with 50 μM TR4 for 30 min and 10 μM DiI in PBS solution for 10 min at 37 °C. (A) CLSM image of TR4 (green, λ_{ex} = 405 nm); (B) CLSM image of DiI (red, λ_{ex} = 543 nm); (C) merged image of panels A and B; (D) 3D luminescence image of panel C.

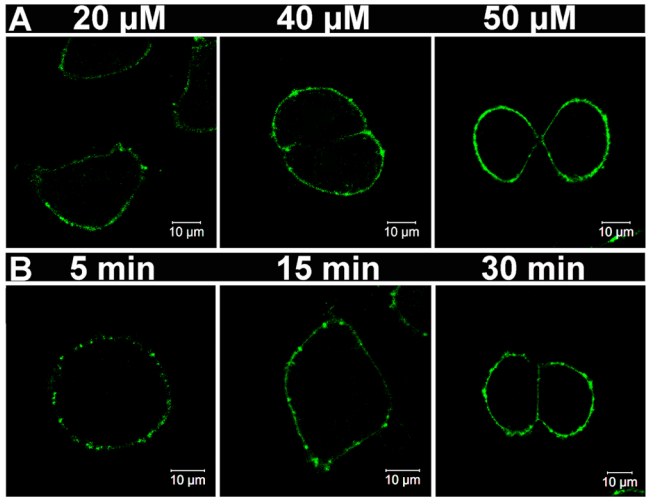

Figure 5. (A) CLSM images of living MCF-7 cells incubated with TR4 at concentrations of 20, 40, and 50 μM for 30 min (green, λ_{ex} = 405 nm); (B) CLSM images of living MCF-7 cells incubated with TR4 (50 μM) (green, λ_{ex} = 405 nm) for 5, 15, and 30 min.

was markedly strengthened. The reason for this is that after insertion of TR4 into the liposomes, the alkyl chains of the lipid bilayer restricted the rotation of the peripheral phenyl rings of TPE.

As a proof-of-concept study, TR4 (50 μM) was incubated with MCF-7 cells to investigate its properties as a cell membrane tracker. When viewed by confocal laser scanning microscopy (CLSM), untreated MCF-7 cells showed negligible background fluorescence. However, after incubating live MCF-7 cells with TR4, bright fluorescence was observed around the cell membrane (green color; Figure 4A). No fluorescent signal was visible in the nucleus and cytoplasm. To further confirm the identity of the fluorescent region, the cell membrane was specifically labeled using a commercial cell membrane tracker (DiI; red color), as shown in Figure 4B. By merging the imaged region, the green TR4 signal was found to colocalize with the red DiI signal, providing evidence that TR4 colocalizes with the cytoplasmic membrane (Figure 4C). Furthermore, three-dimensional (3D) visualization also confirmed that only the cell membrane, and not the nucleus or cytoplasm, was stained by TR4 (Figure 4D). These results indicated that TR4 is an alternative fluorescent bioprobe that can specifically stain cell membranes.

Before TR4 can be used as a membrane tracker, two important parameters, dose and staining time, should be investigated. The use of higher tracker concentrations and longer staining times could both contribute to higher fluorescence intensity, but they also increase the risk of the tracker penetrating through the cell membrane into the cytoplasm, which would decrease the S/N ratio. Thus, we first investigated the effect of dose by incubating MCF-7 cells with TR4 at different concentrations (20, 40, and 50 μM) for 30 min, as shown in Figure 5A. As the TR4 concentration increased, the FL intensity of the cell membrane also increased. When MCF-7 cells were incubated with TR4 at a concentration of 20 μM, the distribution of fluorescence in the cytoplasmic membrane was punctate and not continuous. When the concentration increased to 50 μM, the distribution of fluorescence in the cytoplasmic membrane was uniform and continuous. However, interestingly, when the concentration was increased to 70 μM, the nuclear membrane was brightly labeled by TR4 (see the Supporting Information, Figure S4A). Next, we investigated the effect of staining time by incubating MCF-7 cells with TR4 at 50 μM for different times (5, 15, and 30 min), as shown in Figure 5B. The results were similar to the effect of dose in that the FL intensity of the cell membrane was higher and the distribution was more uniform as the labeling time increased. When the incubation time was extended to 60

dx.doi.org/10.1021/am5025897 | ACS Appl. Mater. Interfaces 2014, 6, 8971−8975

min, we also observed that the nuclear membrane was labeled by TR4 (see the Supporting Information, Figure S4B). It seems that TR4 is a suitable bioprobe for tracking the cell membrane and the nuclear membrane together. However, to track the cytoplasmic membrane alone, MCF-7 cells should be incubated with TR4 for 30 min at concentrations under 50 μM. Next, to investigate the universal applicability of TR4 in different cell lines, we incubated TR4 with HepG-2 and HUVEC cells at 50 μM for 30 min and found that the probe could also light up the cytoplasmic membranes of these cells (see the Supporting Information, Figure S5). Subsequently, the cytoxicity of TR4 (0.05−50 μM) toward the MCF-7 cell line was determined by MTT assay and the cellular viability was calculated to be more that 80% in the presence of TR4 (0.05−50 μM) after incubation for 30 min (see the Supporting Information, Figure S6). This result indicated that TR4 has low cytoxicity at the concentrations used for cell staining.

Photostability is an important feature of a probe used for biological applications. The photostability of TR4 and DiI in living cells was investigated by continuous laser exposure using CLSM. After scanning for 9 min, the normalized fluorescence intensity from TR4 was more than 95% of the original intensity, but the normalized fluorescence intensity from DiI was only about 10% (Figure 6). The CLSM images showed a clear

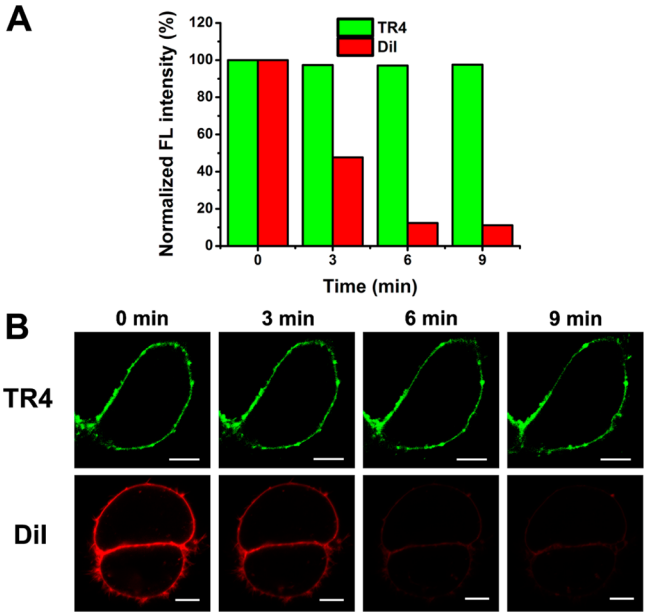

Figure 6. (A) Fluorescence intensity of living MCF-7 cells that were treated with TR4 (green) and DiI (red), then scanned by CLSM for increasing amounts of time (0−9 min); (B) CLSM images of living MCF-7 cells treated with TR4 (green) or DiI (red) with increasing scanning time (0−9 min). Scale bars are 10 μm.

dynamic difference in the fluorescence intensity of TR4 and DiI, and gave strong evidence that TR4 has superior photostability to DiI for bioimaging.

Recently, two-photon microscopy, which employs two near-infrared photos as the excitation source, has attracted more and more attention because of its advantages including deeper tissue penetration, efficient light detection and reduced phototoxicity.[28,29] As previously reported, some TPE-based fluorescent dyes have two-photon absorption characteristics for bioimaging.[30] Therefore, we sought to utilize TR4 as a two-photon bioprobe to track cell membranes by two-photon microscopy. Using 700 nm two-photon microscopy excitiation in scanning lambda mode, the cytoplasmic membranes of TR4-labeled HUVEC cells exhibited intense fluorescence (green color) (see the Supporting Information, Figure S7). This gives TR4 a further advantage over traditional cell membrane dyes.

In summary, we demonstrated the RIR characteristics of TR4 and utilized it as a fluorescence bioprobe for tracking cell membranes. The RIR characteristic was confirmed by the photophysical properties of TR4, which showed high fluorescence intensity in the aggregated state and strong emission after insertion into liposomes in its monodisperse state. Based on these studies, TR4 was utilized to specifically illuminate cell membranes. It showed universal applicability in different cell lines and was highly photostable. Furthermore, the two-photon excitation characteristic of TR4 opens up many new strategies for tracking cell membranes in bioimaging studies.

■ ASSOCIATED CONTENT

Supporting Information

Synthesis and characterization of TR4, dynamic light scattering, emission spectra, CLSM images, cytotoxicity studies, and two-photon microscopy. This material is available free of charge via the Internet at http://pubs.acs.org.

■ AUTHOR INFORMATION

Corresponding Authors

*E-mail: zougz@nanoctr.cn. Fax: +86-010-62656765. Tel: +86-010-82545530 (G.Z.).

*E-mail: liangxj@nanoctr.cn (X.-J.L.).

Notes

The authors declare no competing financial interest.

■ ACKNOWLEDGMENTS

This work was financially supported in part by grants from the State High-Tech Development Plan (2012AA020804), National Natural Science Foundation of China (30970784, 31170873, 21273053, and 81171455), National Key Basic Research Program of China (2009CB930200 and 2012AA022502), and National Distinguished Young Scholars grant (31225009).

■ REFERENCES

(1) Yang, Y.; Zhao, Q.; Feng, W.; Li, F. Luminescent Chemodosimeters for Bioimaging. *Chem. Rev.* **2013**, *113*, 192−270.

(2) Zhao, J.; Wu, W.; Sun, J.; Guo, S. Triplet Photosensitizers: from Molecular Design to Applications. *Chem. Soc. Rev.* **2013**, *42*, 5323−5351.

(3) Jiang, Q. Y.; Lai, L. H.; Shen, J.; Wang, Q. Q.; Xu, F. J.; Tang, G. P. Gene Delivery to Tumor Cells by Cationic Polymeric Nanovectors Coupled to Folic Acid and the Cell-Penetrating Peptide Octaarginine. *Biomaterials* **2011**, *32*, 7253−7262.

(4) Liu, M.; Li, Z. H.; Xu, F. J.; Lai, L. H.; Wang, Q. Q.; Tang, G. P.; Yang, W. T. An Oligopeptide Ligand-Mediated Therapeutic Gene Nanocomplex for Liver Cancer-Targeted Therapy. *Biomaterials* **2012**, *33*, 2240−2250.

(5) Hong, Y.; Lam, J. W.; Tang, B. Z. Aggregation-Induced Emission. *Chem. Soc. Rev.* **2011**, *40*, 5361−5388.

(6) Ding, D.; Li, K.; Liu, B.; Tang, B. Z. Bioprobes Based on AIE Fluorogens. *Acc. Chem. Res.* **2013**, *46*, 2441−2453.

(7) Wang, F.; Wen, J.; Huang, L.; Huang, J.; Ouyang, J. A Highly Sensitive "Switch-on" Fluorescent Probe for Protein Quantification and Visualization Based on Aggregation-Induced Emission. *Chem. Commun.* **2012**, *48*, 7395−7397.

(8) Huang, X.; Gu, X.; Zhang, G.; Zhang, D. A Highly Selective Fluorescence Turn-on Detection of Eyanide Based on the Aggregation of Tetraphenylethylene Molecules Induced by Chemical Reaction. *Chem. Commun.* **2012**, *48*, 12195−12197.
(9) Leung, C. W.; Hong, Y.; Hanske, J.; Zhao, E.; Chen, S.; Pletneva, E. V.; Tang, B. Z. Superior Fluorescent Probe for Detection of Cardiolipin. *Anal. Chem.* **2014**, *86*, 1263−1268.
(10) Li, C.; Wu, T.; Hong, C.; Zhang, G.; Liu, S. A General Strategy to Construct Fluorogenic Probes from Charge-Generation Polymers (CGPs) and AIE-Active Fluorogens through Triggered Complexation. *Angew. Chem., Int. Ed.* **2012**, *51*, 455−459.
(11) Zhao, Q.; Li, K.; Chen, S.; Qin, A.; Ding, D.; Zhang, S.; Liu, Y.; Liu, B.; Sun, J.; Tang, B. Aggregation-Induced Red-NIR Emission Organic Nanoparticles as Effective and Photostable Fluorescent Probes for Bioimaging. *J. Mater. Chem.* **2012**, *22*, 15128−15135.
(12) Zhang, X.; Zhang, X.; Tao, L.; Chi, Z.; Xu, J.; Wei, Y. Aggregation Induced Emission-Based Fluorescent Nanoparticles: Fabrication Methodology and Biomedical Application. *J. Mater. Chem. B* **2014**, DOI: 10.1039/C4TB00291A (Accessed 20th May 2014).
(13) Zhang, X.; Liu, M.; Yang, B.; Zhang, X.; Wei, Y. Tetraphenylethene-Based Aggregation-Induced Emission Fluorescent Organic Nanoparticles: Facile Preparation and Cell Imaging Application. *Colloids Surf. B Biointerfaces.* **2013**, *112*, 81−86.
(14) Zhang, C.; Liu, C.; Xue, X.; Zhang, X.; Huo, S.; Jiang, Y.; Chen, W. Q.; Zou, G.; Liang, X. J. Salt-Responsive Self-Assembly of Luminescent Hydrogel with Intrinsic Gelation-Enhanced Emission. *ACS Appl. Mater. Interfaces.* **2014**, *6*, 757−762.
(15) Zhao, Z.; Lam, J. W.; Chan, C. Y.; Chen, S.; Liu, J.; Lu, P.; Rodriguez, M.; Maldonado, J. L.; Ramos-Ortiz, G.; Sung, H. H.; Williams, I. D.; Su, H.; Wong, K. S.; Ma, Y.; Kwok, H. S.; Qiu, H.; Tang, B. Z. Stereoselective Synthesis, Efficient Light Emission, and High Bipolar Charge Mobility of Chiasmatic Luminogens. *Adv. Mater.* **2011**, *23*, 5430−5435.
(16) Zhang, X.; Chi, Z.; Li, H.; Xu, B.; Li, X.; Zhou, W.; Liu, S.; Zhang, Y.; Xu, J. Piezofluorochromism of an Aggregation-Induced Emission Compound Derived from Tetraphenylethylene. *Chem-Asian. J.* **2011**, *6*, 808−811.
(17) Zhang, X.; Chi, Z.; Xu, B.; Chen, C.; Zhou, X.; Zhang, Y.; Liu, S.; Xu, J. End-Group Effects of Piezofluorochromic Aggregation-Induced Enhanced Emission Compounds Containing Distyrylanthracene. *J. Mater. Chem.* **2012**, *22*, 18505−18513.
(18) Zhang, X.; Chi, Z.; Zhang, Y.; Liu, S.; Xu, J. Recent Advances in Mechanochromic Luminescent Metal Complexes. *J. Mater. Chem. C* **2013**, *1*, 3376−3390.
(19) Geng, J.; Li, K.; Ding, D.; Zhang, X.; Qin, W.; Liu, J.; Tang, B. Z.; Liu, B. Lipid-PEG-Folate Encapsulated Nanoparticles with Aggregation Induced Emission Characteristics: Cellular Uptake Mechanism and Two-Photon Fluorescence Imaging. *Small* **2012**, *8*, 3655−3663.
(20) Hong, Y.; Lam, J. W.; Tang, B. Z. Aggregation-Induced Emission: Phenomenon, Mechanism and Applications. *Chem. Commun.* **2009**, 4332−4353.
(21) Xue, X.; Zhao, Y.; Dai, L.; Zhang, X.; Hao, X.; Zhang, C.; Huo, S.; Liu, J.; Liu, C.; Kumar, A.; Chen, W. Q.; Zou, G.; Liang, X. J. Spatiotemporal Drug Release Visualized through a Drug Delivery System with Tunable Aggregation-Induced Emission. *Adv. Mater.* **2014**, *26*, 712−717.
(22) Zhang, C.; Jin, S.; Li, S.; Xue, X.; Liu, J.; Huang, Y.; Jiang, Y.; Chen, W. Q.; Zou, G.; Liang, X. J. Imaging Intracellular Anticancer Drug Delivery by Self-Assembly Micelles with Aggregation-Induced Emission (AIE Micelles). *ACS Appl. Mater. Interfaces.* **2014**, *6*, 5212−5220.
(23) Shi, H.; Liu, J.; Geng, J.; Tang, B. Z.; Liu, B. Specific Detection of Integrin $\alpha_V\beta_3$ by Light-up Bioprobe with Aggregation-Induced Emission Characteristics. *J. Am. Chem. Soc.* **2012**, *134*, 9569−9572.
(24) Leung, C. W.; Hong, Y.; Chen, S.; Zhao, E.; Lam, J. W.; Tang, B. Z. A Photostable AIE Luminogen for Specific Mitochondrial Imaging and Tracking. *J. Am. Chem. Soc.* **2013**, *135*, 62−65.
(25) Li, Y.; Wu, Y.; Chang, J.; Chen, M.; Liu, R.; Li, F. A Bioprobe Based on Aggregation Induced Emission (AIE) for Cell Membrane Tracking. *Chem. Commun.* **2013**, *49*, 11335−11337.
(26) Wang, E.; Zhao, E.; Hong, Y.; Lam, J.; Tang, B. A Highly Selective AIE Fluorogen for Lipid Droplet Imaging in Live Cells and Green Algae. *J. Mater. Chem. B* **2014**, *2*, 2013−2019.
(27) Gao, M.; Hu, Q.; Feng, G.; Tang, B.; Liu, B. A Fluorescent Light-up Probe with "AIE + ESIPT" Characteristics for Specific Detection of Lysosomal Esterase. *J. Mater. Chem. B* **2014**, *2*, 3438−3442.
(28) Zipfel, W. R.; Williams, R. M.; Webb, W. W. Nonlinear Magic: Multiphoton Microscopy in the Biosciences. *Nat. Biotechnol.* **2003**, *21*, 1369−1377.
(29) Kim, H. M.; Cho, B. R. Two-Photon Probes for Intracellular Free Metal Ions, Acidic Vesicles, and Lipid Rafts in Live Tissues. *Acc. Chem. Res.* **2009**, *42*, 863−872.
(30) Hu, R.; Maldonado, J.; Rodriguez, M.; Deng, C.; Jim, C.; Lam, J.; Yuen, M.; Ramos-Ortiz, G.; Tang, B. Z. Luminogenic Materials Constructed from Tetraphenylethene Building Blocks: Synthesis, Aggregation-Induced Emission, Two-Photon Absorption, Light Refraction, and Exposive Detection. *J. Mater. Chem.* **2012**, *22*, 232−240.